Geobios 46 (2013) 539–548

Available online at
ScienceDirect
www.sciencedirect.com

Elsevier Masson France
EM|consulte
www.em-consulte.com

Original article

A juvenile skull of *Acerorhinus yuanmouensis* (Mammalia: Rhinocerotidae) from the Late Miocene hominoid fauna of the Yuanmou Basin (Yunnan, China)☆

Xiaokang Lu [a,b,*]

[a] *Key Laboratory of Vertebrate Evolution and Human Origins of the Chinese Academy of Sciences, Institute of Vertebrate Paleontology and Paleoanthropology, Chinese Academy of Sciences, Beijing 100044, China*
[b] *University of the Chinese Academy of Sciences, Beijing 100049, China*

ARTICLE INFO

Article history:
Received 4 February 2013
Accepted 10 October 2013
Available online 23 October 2013

Keywords:
Acerorhinus
Aceratheriinae
Ontogeny
Cladistic analysis
Late Miocene
Yuanmou
Hominoid fauna

ABSTRACT

A unique juvenile skull bearing both milk premolars and unerupted but fully developed permanent premolars and molars (observed using X-ray microcomputed tomography), and some isolated upper cheek teeth, all from the Late Miocene hominoid fauna of the Yuanmou Basin (Yunnan, China), closely resemble craniodental material of *Acerorhinus yuanmouensis* Zong, 1998 from the same locality, and are referred to this species. A phylogenetic analysis based on 214 craniodental morphological characters scored for 31 terminal taxa reveals that *A. yuanmouensis* should be assigned to the genus *Acerorhinus* indeed. The newly discovered specimens improve our understanding of this species, especially with respect to the morphology of the milk premolars and premolars. Two intraspecific variations in the upper premolars are noted: a lingual bridge may be present or absent, and the lingual cingulum continuous or reduced. The analysis also indicates that: the phylogenetic status of *Acerorhinus lufengensis* Deng and Qi, 2009 should be reconsidered; "*Aceratherium*" *huadeensis* Qiu, 1979 does neither belong to *Aceratherium* nor *Acerorhinus*, and its phylogenetic status remains debatable.

1. Introduction

The Yuanmou Basin, containing sites that have yielded the Late Miocene hominoid *Lufengpithecus*, lies on the northern edge of the Yunnan-Guizhou Plateau in the Yunnan Province, China (Jiang et al., 1987, 1993; Jiang, 1997; Kelley and Gao, 2012) (Fig. 1). The basin contains typical diluvial-alluvial deposits indicative of strong seasonality, comprising mainly purple siltstones and pebbly fine sandstones with some yellow gravel lenticular bodies (Zhang et al., 2002). The micromammalian fauna indicates an age of about 9 Ma (Ni and Qiu, 2002), slightly older than the 7–8 Ma indicated by paleomagnetic data (Yue et al., 2004). The Yuanmou hominoid fauna points to a humid environment dominated by montane forests with luxuriant shrubs, patches of open grasslands, and a nearby water source (Ni and Qiu, 2002; Qi et al., 2006). The Xiaohe area of the Yuanmou Basin has yielded numerous fossil mammals, including *Lufengpithecus*, *Hipparion* and *Tetralophodon* (Jiang, 1996; Pan, 1997). Among them are two aceratheriine genera, *Subchilotherium* and *Acerorhinus*.

Acerorhinus was established by Kretzoi (1942) based on the species "*Aceratherium*" *zernowi* (Borissiak, 1914) from the Sevastopol *Hipparion* fauna of Crimea, Ukraine. Heissig (1975) assigned *Acerorhinus* to *Chilotherium* as a subgenus, and referred three additional species to it. Qiu et al. (1987) reestablished *Acerorhinus* at the genus rank within tribe Chilotheriini Qiu et al., 1987.

Cerdeño (1996) noted the occurrence of *Acerorhinus zernowi* in the Middle Miocene Tung-gur Formation of Inner Mongolia, China. This referral was discounted by Deng (2000). Antoine et al. (2003) referred *Alicornops alfambrense* Cerdeño and Alcalá, 1989 to *Acerorhinus* as *A. alfambrense*. Deng and Qi (2009) recognized six species within the genus *Acerorhinus*: *A. zernowi* (Borissiak, 1914); *A. palaeosinensis* (Ringström, 1924); *A. tsaidamensis* (Bohlin, 1937); *A. hezhengensis* Qiu et al., 1987; *A. fuguensis* Deng, 2000; and *A. lufengensis* Deng and Qi, 2009. Deng et al. (2013) recently referred "*Aceratherium*" *huadeensis* Qiu, 1979 from the Late Miocene of Inner Mongolia, China, to *Acerorhinus* as *A. huadeensis* (Qiu, 1979).

Two species of *Acerorhinus* have been reported within the Yuanmou hominoid fauna, namely "*Acerorhinus xiaoheensis*" Gao and Ma, 1997, and *Acerorhinus yuanmouensis* Zong, 1998. Deng (2000) synonymized the latter with the former. Deng and Gao (2006) subsequently referred "*Acerorhinus xiaoheensis*" to *Subchilotherium intermedium* (Lydekker, 1881). Since that, the phylogenetic status of *A. yuanmouensis* has not been discussed. In this study, a juvenile skull and a few isolated teeth from the Yuanmou hominoid fauna are used

☆ Corresponding editor: Pierre-Olivier Antoine.

* Key Laboratory of Vertebrate Evolution and Human Origins of the Chinese Academy of Sciences, Institute of Vertebrate Paleontology and Paleoanthropology, Chinese Academy of Sciences, Beijing 100044, China.
E-mail address: luxiaokang@ivpp.ac.cn.

0016-6995/$ – see front matter © 2013 Elsevier Masson SAS. All rights reserved.
http://dx.doi.org/10.1016/j.geobios.2013.10.001

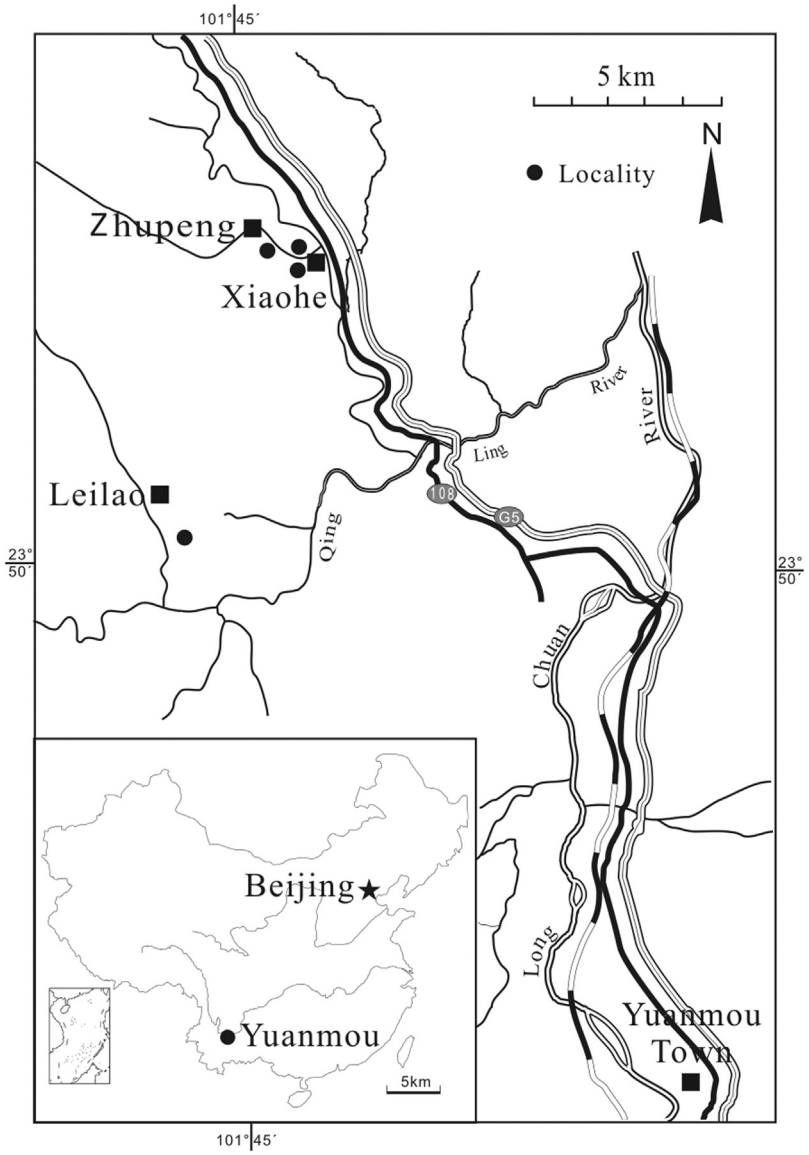

Fig. 1. Location of the Late Miocene of the Yuanmou Basin in Yunnan, China.

as a basis for discussing the validity of *A. yuanmouensis*, and discussing the phylogenetic relationships among Chinese species of *Acerorhinus*.

The terminology and taxonomy used in this paper follow Sisson (1953), Heissig (1989), Prothero and Schoch (1989), and Antoine (2002). Measurements (in mm) follow the protocol of Guérin (1980).

Abbreviations: GSMV, Gansu Museum, Lanzhou, China; IVPP V or RV, Institute of Vertebrate Paleontology and Paleoanthropology, Beijing, China; PDYV, fossils from the Yuanmou Basin stored in the Yunnan Institute of Cultural Relics and Archaeology, Kunming, China; PMU or M, Evolutionsmuseet, University of Uppsala, Uppsala, Sweden; YZ, fossils from the Yuanmou Basin stored in the State Museum of Chuxiong, Yunnan, China.

2. Methods

2.1. CT scanning

Images of the unerupted but fully developed P2-P4 and M1-M2 of V18565 were acquired through X-ray microcomputed tomography, using the 450 kV industrial CT (developed by the Institute of High Energy Physics, CAS) at the Key Laboratory of Vertebrate Evolutionary and Human Origins in the IVPP. The specimen was scanned using a fan beam energy of 430 kV and 1.6 mA. Based on a slice distance of 0.3 mm, a total of 860 transmission images with dimensions of 2048 × 2048 pixels and a pixel size of 0.2 mm were generated using 2D image processing software developed by the Institute of High Energy Physics, CAS. 3D reconstructions were created using Mimics v.14.12, and images of the reconstructions were exported from Mimics and finalized with Adobe Photoshop.

This technique makes it possible to observe the morphology of the permanent premolars P2-P4 and molars M1-M3. Unfortunately, the crown of M3 is only partly formed, being only half as high as expected despite having normal length and breadth; its morphological features are neither described nor discussed here. The P2-P4 and M1-M2 were reconstructed using special software, and the reconstructed teeth were drawn. Measurements of reconstructed teeth were taken using Mimics.

2.2. Phylogenetic analysis

An analysis was carried out using the craniodental data matrix of Antoine (2002) and Antoine et al. (2003, 2010), with 32 newly

added characters (18 cranial, 4 mandibular, 10 dental). Therefore, a total of 214 characters (70 cranial, 14 mandibular, and 130 dental) were included in the data matrix used in the present paper (Appendix A-2). The following paragraphs provide brief comments on some of the newly added characters.

All characters were equally weighted. A total of 10 characters, including four (94, 123, 131, 170) from the original data matrix of Antoine (2002) and six (2, 3, 8, 30, 31, 65) newly added, were treated as unordered, whereas all other 204 characters were ordered. Gaps were treated as 'missing'. The analysis was carried out with PAUP 4.0β10 (Swofford, 2001), using a heuristic search, branch swapping TBR, and with a random addition sequence.

Thirty-one terminal taxa were included in the phylogenetic analysis (Appendix A-1). The stem rhinocerotid *Trigonias osborni* Lucas, 1901 from the Eocene of North America was designated as the outgroup. Thirteen taxa were added with respect to previous studies:

- the earliest known aceratheriine in China, *Plesiaceratherium* Young, 1937, with *P. gracile* Young, 1937 from the late Early Miocene of China;
- the monotypic genus *Subchilotherium*, with *S. intermedium* from Middle to Late Miocene of Pakistan and China;
- the most widely distributed aceratheriine in Eurasia, *Chilotherium* Ringström (1924), with *C. wimani* and *C. anderssoni* from the Late Miocene of Eurasia;
- *Acerorhinus* Kretzoi, 1942, with *A. yuanmouensis* Zong, 1998, *A. zernowi* (Borissiak, 1914), *A. palaeosinensis* (Ringström, 1924), *A. tsaidamensis* (Bohlin, 1937), *A. hezhengensis* Qiu et al., 1987, *A. fuguensis* Deng, 2000, and *A. lufengensis* Deng and Qi, 2009, from the Late Miocene of Eurasia;
- "*Aceratherium*" *huadeensis* Qiu, 1979, from the Late Miocene of Inner Mongolia, China;
- probably the latest appearing aceratheriine, *Shansirhinus* Kretzoi, 1942, with *S. ringstroemi* Kretzoi, 1942 from the Pliocene of China.

Acerorhinus alfambrense (Cerdeño and Alcalá, 1989) was not included in the present analysis due to the lack of direct observation.

Codings for the Chinese taxa were based on direct observation of specimens except in the cases of *A. zernowi*, *A. palaeosinensis*, and *S. intermedium*, for which coding was partly based on the literature. Scoring for other taxa was taken from Antoine (2002) and Antoine et al. (2003, 2010) for the 182 craniodental characters originally present in the matrix, and was based on the literature for the 32 newly added characters. The data matrix is presented in Appendix A-4. Some notes on individual new characters in the matrix follow.

Character 6. Infraorbital foramen: 0, one; 1, two-three. Ordered. Qiu et al. (1982) noted the presence of multiple infraorbital foramina in *Shansirhinus*, *Chilotherium* and *Acerorhinus*.

Character 9. Nasal notch, distance to the orbit relative to the length of skull: 0, long (> 17%); 1, short (≤ 17%). Ordered. Yan and Heissig (1986) noted the short distance between the orbit and the nasal notch in *Plesiaceratherium*. The two structures are even closer together in the more advanced aceratheriines *Acerorhinus* and *Shansirhinus* (Qiu et al., 1987; Deng, 2005). The different states are defined according to the proportion of the distance between the orbit and the nasal notch relative to the length from the occipital condyle to the premaxillary bone.

Character 19. Zygomatic arches, depression at the external surface of the anterior part: 0, absent; 1, present. Ordered. When present, the depression is round in outline and close to the posterior rim of the orbit.

Character 36. Skull, narrowing of the dorsal surface anterior to the orbit: 0, gradual; 1, sharp. Ordered. Sharp constriction of the dorsal surface of the skull anterior to the orbit was reported in *Aceratherium incisivum* by Yan and Heissig (1986), in *Acerorhinus* by Heissig (1999), and in *S. ringstroemi* by Deng (2005).

Character 37. Skull, widest part of the dorsal surface: 0, at level of postorbital process; 1, at level of supraorbital process. Ordered. Qiu et al. (1987) mentioned that in *A. hezhengensis* the maximum width of the dorsal surface of the skull occurs at level of the supraorbital processes.

Character 51. Parietal crest, dorsal surface: 0, concave; 1, prominent. Ordered. On dorsal view, the joint between the parietal crest and the occipital crest is prominent. On lateral view, the height of the parietal crest is flushing with the occipital crest anterior to the V-shaped incision.

Character 65. Nuchal face, outline: 0, bell-shaped; 1, trapezoidal; 2, square. Unordered. Qiu et al. (1987) noted that in *Acerorhinus* the nuchal face of the skull is bell-shaped in outline.

Character 73. Symphysis, ventral surface: 0, flat; 1, concave. Ordered. This corresponds to the description by Deng (2005).

Character 81. Mandible, orientation of row of lower cheek teeth: 0, not parallel to long axis of mandible; 1, parallel to long axis of mandible. Ordered. In *S. ringstroemi*, the lower cheek teeth row is nearly in line with the long axis of the horizontal part of the mandibular ramus (Deng, 2005).

Character 103. i2, upturning of the internal edge: 0, absent; 1, present. Ordered. In both *Chilotherium wimani* (Deng, 2001a) and *A. lufengensis* (Deng and Qi, 2009) the internal edge of i2 is upturned at the upper part of the crown.

Character 106. Upper cheek teeth, lingual rim of row of upper cheek teeth: 0, arched; 1, always straight. Ordered. In *A. hezhengensis*, P4-M2 have expanded lingual cusps and widened crowns, and the lingual rim of this tooth series forms a straight line (Qiu et al., 1987).

Character 107. Upper cheek teeth, branch of the crochet: 0, always absent; 1, occasionally present; 2, always present. Ordered. Kretzoi (1942) used the presence of the branched crochet or crista on the upper cheek teeth to establish the genus *Shansirhinus*.

Character 109. Upper cheek teeth,lingual cusps: 0, expanded; 1, unexpanded. Ordered. Deng (2000) indicated that the two lingual cusps (protocone and hypocone) are expanded on the upper cheek teeth of *A. fuguensis*.

3. Systematic paleontology

Order PERISSODACTYLA Owen, 1848
Family RHINOCEROTIDAE Gill, 1872
Subfamily ACERATHERIINAE Dollo, 1885
Tribe CHILOTHERIINI Qiu et al., 1987
Genus ***Acerorhinus*** Kretzoi, 1942
Acerorhinus yuanmouensis Zong, 1998

Figs. 2–5

Holotype: YZ 006, well-preserved adult skull with badly worn upper cheek teeth, from the Xiaohe Formation of the Yuanmou Basin (Zong, 1998: figs. 1 and 2; Table 1).

Paratype: YZ 007, right M1. Same provenance as the holotype.

Studied material: IVPP V18565 (Figs. 2–4; Tables 1 and 2), skull, with postcranial bones not included in this study; PDYV 0610, right DP3 (Fig. 5(A)); PDYV 0413, left DP4 (Fig. 5(B)); PDYV 0175, left P4 (Fig. 5(C)); PDYV 0096, left M1 (Fig. 5(D)); PDYV 0269, left M2 (Fig. 5(E)). All specimens recovered from the Upper Miocene Xiaohe Formation (MN11-MN12) of Yuanmou Basin, Yunnan, China.

Geographic distribution: Xiaohe area, including Xiaohe, Zhupeng and Leilao, Yuanmou County, Yunnan Province, China (Zong, 1998) (Fig. 1).

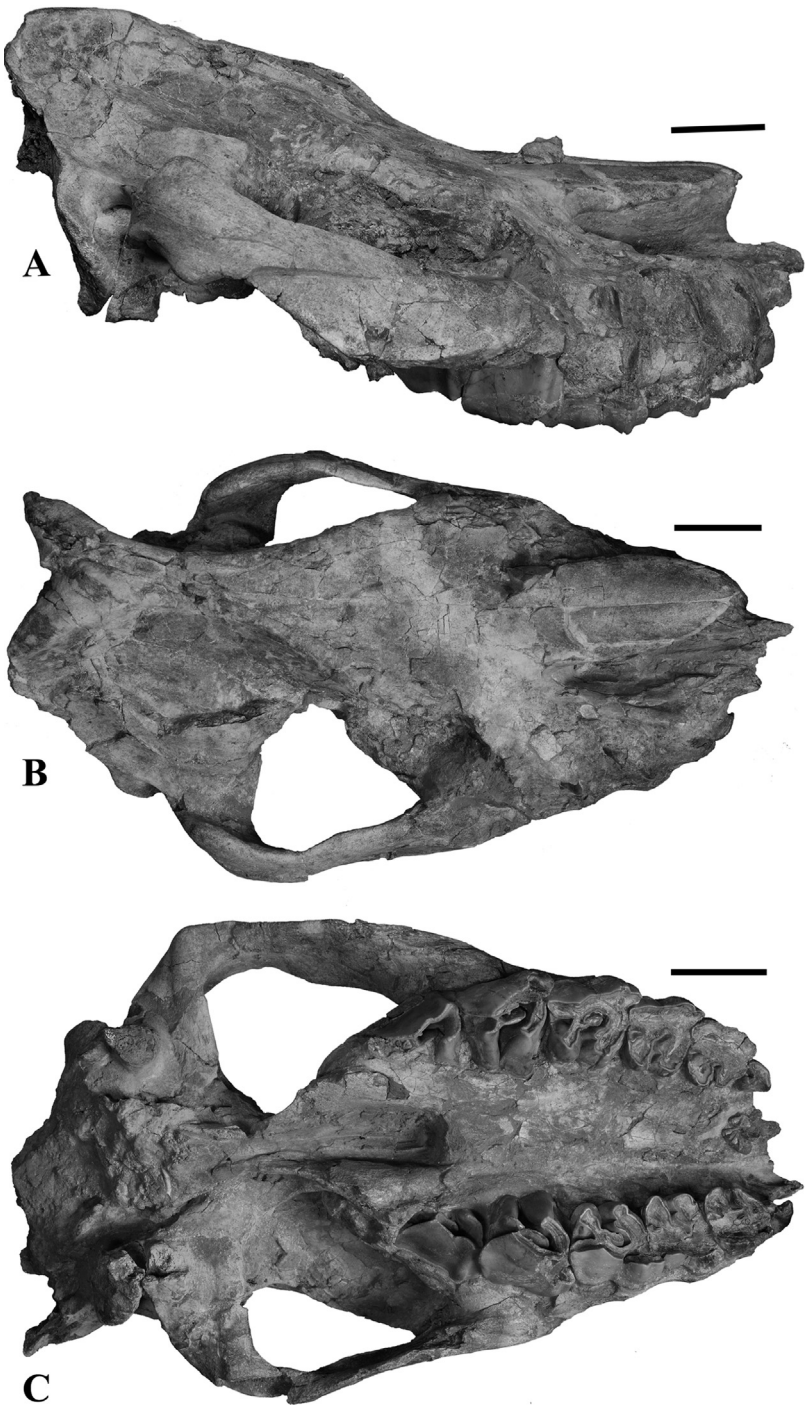

Fig. 2. *Acerorhinus yuanmouensis*, IVPP V 18565, Late Miocene, Yuanmou Basin (Yunnan, China): skull. **A**: lateral view; **B**: dorsal view; **C**: ventral view. Scale bars: 50 mm.

Fig. 3. *Acerorhinus yuanmouensis*, IVPP V 18565, Late Miocene, Yuanmou Basin (Yunnan, China): DP1-M2 in occlusal view. Scale bar: 50 mm.

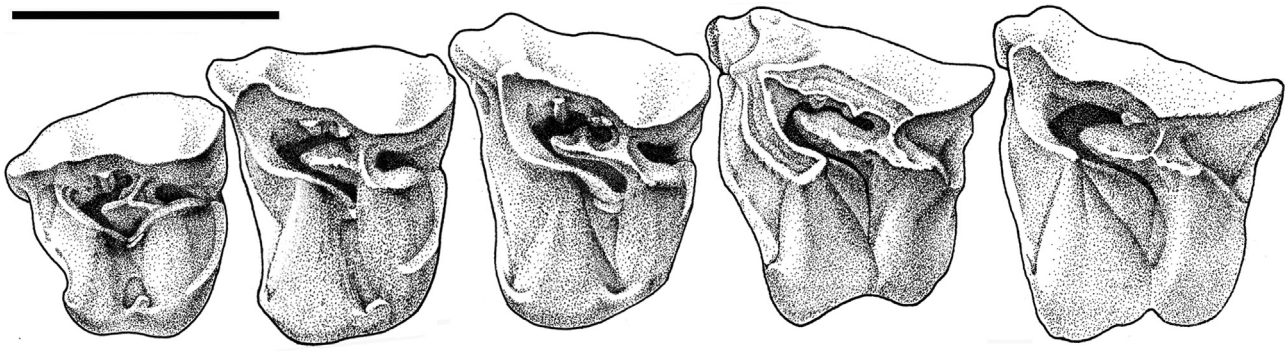

Fig. 4. *Acerorhinus yuanmouensis*, IVPP V 18565, Late Miocene, Yuanmou Basin (Yunnan, China): drawing of P2-M2 based on the reconstruction of right upper cheek teeth. Scale bar: 50 mm.

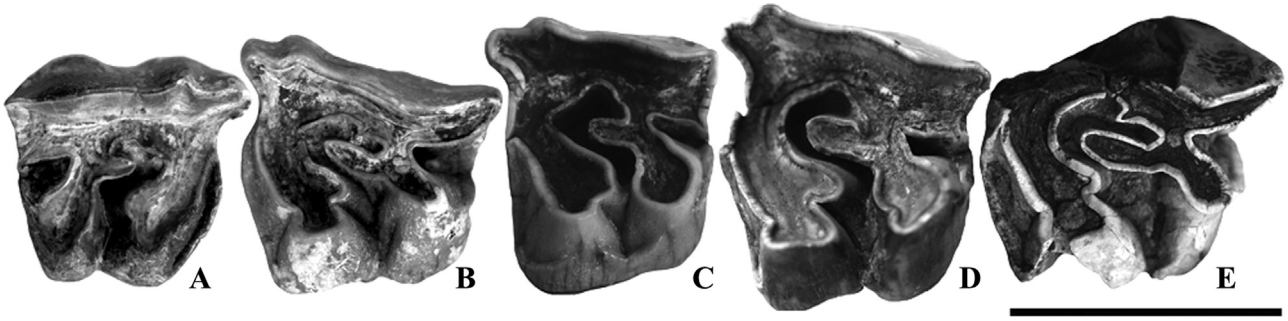

Fig. 5. Isolated upper cheek teeth of *Acerorhinus yuanmouensis* from the Late Miocene Yuanmou Basin (Yunnan, China). **A**: PDYV 0610, right DP3; **B**: PDYV 0413, left DP4; **C**: PDYV 0175, left P4; **D**: PDYV 0096, left M1; **E**: PDYV 0269, left M2. Scale bar: 50 mm.

Table 1
Measurements (in mm) of the skull of *Acerorhinus yuanmouensis* (V18565) from the Late Miocene of the Yuanmou Basin in Yunnan, China, and of the holotype skull of this species as well as skulls of some other species of *Acerorhinus*.

Measures	V18565	*A. yu*	*A. ts*	*A. pa*	*A. fu*
1 Distance between occipital condyle and premaxilla	–	510	516	–	585
2 Distance between occipital condyle and nasal tip	–	–	518	–	–
3 Distance between nasal tip and occipital crest	418	432	492	–	–
4 Distance between nasal tip and bottom of nasal notch	112	110	159	164	–
5 Minimal width of braincase	–	–	10	24	28
6 Distance between occipital crest and postorbital process	224	246	252	–	265
7 Distance between occipital crest and supraorbital process	243	274	264	–	290
8 Distance between occipital crest and lacrimal tubercle	276	300	313	–	328
9 Distance between nasal notch and orbit	58	67	57	71	95
13 Distance between occipital condyle and M3	–	265	249	–	270
14 Distance between nasal tip and orbit	168	163	203	–	–
15 Width of occipital crest	–	–	119	129	162
16 Width of paramastoid process	–	172	186	189	216
17 Minimal width between parietal crests	33	36	10	24	28
18 Width between postorbital processes	115	–	148	–	165
19 Width between supraorbital processes	129	–	166	150	183
20 Width between lacrimal tubercles	124	–	154	–	178
21 Maximal width between zygomatic arches	247	–	293	273	267
22 Width of nasal base	104	103	83	95	84
23 Height of occipital surface	–	153	151	–	140
25 Cranial height in front of P2	–	–	117	–	113
26 Cranial height in front of M1	–	–	158	–	146
27 Cranial height in front of M3	–	–	169	–	146
28 Width of palate in front of P2	54	61	49	–	60
29 Width of palate in front of M1	77	66	60	–	86
30 Width of palate in front of M3	100	75	68	–	89
31 Width of foramen magnum	–	–	40	34	45
32 Width between exterior edges of occipital condyle	–	105	121	104	118

A. yu: *A. yuanmouensis*, YZ 006, from the Late Miocene of the Yuanmou Basin in Yunnan, China (Zong, 1998); *A. ts*: *A. tsaidamensis*, RV 37009, from the Late Miocene of the Qaidam Basin in Qinghai, China (Bohlin, 1937: pp. 64–65); *A. pa*: *A. palaeosinensis*, M 3880, from the Late Miocene in Baode, Shanxi, China (Bohlin, 1937: pp. 64–65); *A. fu*: *A. fuguensis*, V 11963, from the Late Miocene in Fugu, Shaanxi, China (Deng, 2000: table 2).

Table 2
Measurements (length/width, in mm) of the upper cheek teeth of *Acerorhinus yuanmouensis* (V18565) from the Late Miocene of the Yuanmou Basin in Yunnan, China, and of the teeth of the holotype of this species as well as those of other species of *Acerorhinus*.

Measures	V18565	*A. yu*	*A. lu*	*A. ts*	*A. pa*	*A. fu*	*A. he*
DP1	23/20	–	–	20/17	–	–	–
DP2	41/38	–	–	41/38	–	–	–
DP3	42/43	–	–	48/45	–	–	–
DP4	52/49	–	–	55/51	–	–	–
P2	41/46	47/35	–	33/43	35/43	44/45	37/42
P3	44/55	42/57	–	37/59	39/54	45/59	44/51
P4	46/58	41/60	45/58	45/64	42/57	49/65	47/55
M1	52/58	41/62	57/68	51/66	39/59	57/62	57/58
M2	52/59	45/58	59/71	56/66	48/60	62/65	57/58
M3	–	54/53	54/63	58/59	56/55	49/53	49/53
DP1-DP4	130	–	–	–	–	–	–
DP1-M3	–	254	–	246	240	–	–
DP1-P4	–	–	–	125	126	–	–
M1-M3	–	122	–	138	124	–	–
DP1-P4/M1-M3	–	–	–	0.91	1.01	–	–

A. yu: *A. yuanmouensis*, YZ 006, from the Late Miocene of the Yuanmou Basin in Yunnan, China (Zong, 1998); *A. lu*: *A. lufengensis*, V 15980, from the Late Miocene of the Lufeng Basin in Yunnan, China (Deng and Qi, 2009: table 1; *A. ts*: *A. tsaidamensis*, RV 37009, from the Late Miocene of the Qaidam Basin in Qinghai, China (Bohlin, 1937: pp. 64–65); *A. pa*: *A. palaeosinensis*, M 3880, from the Late Miocene in Baode, Shanxi, China (Bohlin, 1937: pp. 64–65); *A. fu*: *A. fuguensis*, V 11963, from the Late Miocene in Fugu, Shaanxi, China (Deng, 2000: table 2); *A. he*: *A. hezhengensis*, GMSV 8001, from the Late Miocene of the Linxia Basin in Gansu, China (Qiu et al., 1987: table 1).

Stratigraphic distribution: Late Miocene, lower Xiaohe Formation, Baodean (East Asian Land Mammal Age) of China, corresponding to the Turolian (MN11- MN12) of Europe (Qiu and Qiu, 1995; Steininger, 1999; Deng, 2006; Qi et al., 2006).

Emended diagnosis: Parietal crests narrow. Nasals extremely short, with an undulating dorsal profile. Nasal notch retracted to level of M1. Cristae on upper cheek teeth always doubled. On upper premolars, lingual bridge variably present and lingual cingulum continuous or reduced.

Description: **skull**: The occipital part of the skull is greatly elevated over the front surface (Fig. 2(A)). The swelling on the frontals and nasals is nearly invisible, so that this part of the skull roof appears approximately flat. The incompletely preserved premaxillae have a dorsoventral depth of 23–25 mm, and are probably edentulous. The widest part of the dorsal surface of the skull is located between the supraorbital processes, and the skull roof narrows abruptly anterior to the orbit (Fig. 2(B); Table 1). The parietal crests approach one another at the level of the posterior end of the zygomatic arches, but never meet to form a sagittal crest. They become prominent as they approach the occiput, so that their dorsal edges are height flush with that of the occipital crest. A V-shaped notch intrudes posteriorly into the occipital crest. Whether the occipital crest extends far enough posteriorly to overhang the occipital condyles is unknown, because the occipital crest is partly distorted and the condyles are missing. On the nuchal face, the only noteworthy feature that remains intact is the depression for insertion of the nuchal ligament.

The nasal is hornless and short (length: 110 mm). Its dorsal surface has an undulating profile: the middle of the bone is slightly concave, in contrast to the flat anterior and posterior parts. The posterior half of the lateral margins droops and curves ventrally. The rostral end of the nasal, at the level of DP2, is narrow. The nasals are totally separated, with an obvious median suture between them. The nasal notch extends back to the level of the posterior rim of DP4. All three infraorbital foramina are below the notch, at the level of DP3-DP4. The largest foramen is situated above the anterior half of DP4, and opens dorsally and anteriorly; the smallest foramen is at the level of the middle of DP3, and continues anteriorly as a straight, short groove; and the last foramen lies on the ventral edge of the notch, and also continues anteriorly but forms a longer groove than does the smallest foramen. The orbit extends anteriorly to the level of the posterior edge of M1, closely approaching the nasal notch (Fig. 2(A)). The frontal and zygomatic arches lack the postorbital processes, but the supraorbital process on the frontal is large and rough.

The zygomatic arches are dorso-ventrally deep (75–80 mm). No posterior process is present on the dorsal rim of the arch, but one ventral constriction occurs anterior to the temporal condyle. The postglenoid process meets the distal part of the posttympanic process below the exterior auditory pseudo-meatus, but the two processes never fuse one each other. The anteroposteriorly compressed but transversely expanded posttympanic process turns posteriorly and tapers to a point slightly beyond the contact with the postglenoid process.

The narrow and slightly arched posterior rim of the horizontal part of the palatine bone forms the anterior border of the choana, which lies at the level of the anterior part of M2 (Fig. 2(C)). The ventral spine of the vomer is narrow. The anterior part of the foramen lacerum extends anteriorly to the level of the temporal condyle (Fig. 2(C)).

Upper teeth: The milk premolars are badly worn, with the exception of DP1 which is only slightly worn (Fig. 3). The crowns of P2-M2 are slightly wider than long (Figs. 4 and 5; Table 2).

DP1 is simple in morphology, with a convex labial surface. The parastyle is narrower than the protocone and the metacone, and curves slightly anteriorly and lingually. A metaloph and hypocone are present, but there is no protocone or protoloph. The lingual cingulum running from the parastyle becomes separate from the posterior cingulum at the lingual wall of the hypocone. The posterior fossette is nearly closed by the posterior cingulum, and has the outline of a triangle whose apex is directed anteriorly.

On DP2, the crown is worn down almost to the root, but even at this stage the parastyle and the paracone rib remain visible. The hypocone is much larger than the protocone. Neither lingual cusp is constricted (Fig. 3). The anterior cingulum is almost completely fused with the protoloph, although a remnant of an anterior fossette is still present between the two structures. The posterior cingulum is fully fused with the metaloph. The posterior fossette is nearly worn away. A small pillar rather than a lingual cingulum is present at the entrance of the median valley, which remains lingually open. Contact between the crochet and the protoloph has produced a median fossette, which however is nearly worn away.

DP3 and DP4 are closely similar in most respects. The parastyle and paracone rib are better developed on these teeth than on DP2, especially on the slightly worn teeth PDYV 0610 (DP3; length/width = 42/40 mm) and PDYV 0413 (DP4; length/width = 50/50 mm) (Fig. 5(A, B)). The metastyle is less elongated on DP3 than

on DP4. The constrictions on both lingual cusps are much deeper on DP3 and DP4 than on DP2 (Fig. 3). The crochet runs anteriorly and labially, paralleling the ectoloph and intersecting medially with the short antecrochet to nearly close off the median valley. The crista is absent. The anterior cingulum ends at the lingual wall of the protoloph. The posterior cingulum is reduced to a V-shaped ledge around the opening of the posterior fossette. There is no lingual cingulum, but a pillar is present at the entrance of the median valley.

The following description of the upper cheek teeth is based on the reconstructed morphology of P2-M2 in the skull IVPP V 18565 (Fig. 4), and also on three isolated cheek teeth (Fig. 5(C-E)).

On P2, the parastyle and paracone rib are similar to the equivalent structures on DP2, but the metastyle is absent. The protocone is less well developed than the hypocone, but the two are linked by a high lingual bridge. Neither of the lingual cusps is constricted (Fig. 4). The protoloph contacts the ectoloph. The crochet fails to contact the crista, and no median fossette is present. Remnants of the lingual cingulum persist at the entrance of the median valley. The V-shaped posterior cingulum extends around the posterior valley.

P3 and P4 resemble P2 in most respects, but have some features that give them a more molariform occlusal pattern: the protocone and the protoloph are larger and longer than the hypocone and the metaloph, respectively; the metastyle extends farther posteriorly than in P2, and curves labially; the protocone and hypocone are constricted (Fig. 4); the crista is consistently present except in PDYV 0175 (P4; length/width = 43/52 mm; Fig. 5(C)); and the crochet runs parallel to the ectoloph. PDYV 0175 resembles the holotype specimen YZ 006 in lacking a lingual bridge.

M1 and M2 are similar to one another. In these teeth the parastyle and paracone rib are well developed. The metastyle extends farther posteriorly than in P2-P4 and DP2-DP4. The degree of constriction of both lingual cusps is greater than in P3-P4 (Fig. 4), but about the same as in DP3 and DP4. The antecrochet is as long as in DP3 and DP4. Both M1 and M2 bear one or two weak cristae, although PDYV 0096 (M1; length/width = 50/55 mm; Fig. 5(D)) lacks cristae. The anterior and posterior cingula are as strongly reduced as in DP3 and DP4, and no lingual cingulum is present. M2 differs from M1 only in having a more elongated metastyle.

Remarks: Judging by established criteria for assessing biological age for extant or extinct rhinoceros (Goddard, 1970; Hitchins, 1978; Hillman-Smith et al., 1986; Deng, 2001b), the new juvenile skull specimen of *A. yuanmouensis* is probably from an individual 3.5–4 years old given its slightly worn M1, erupting M2 and badly worn but still present milk premolars. The holotype of *A. yuanmouensis*, which has badly worn upper cheek teeth, represents an old individual (Zong, 1998).

Two aceratheriines have been described from the Late Miocene Yuanmou Basin in Yunnan, China: "*Acerorhinus xiaoheensis*" Gao and Ma, 1997, and *A. yuanmouensis* Zong, 1998.

The former species was referred to *Subchilotherium intermedium* by Deng and Gao (2006). Gao and Ma (1997) established "*Acerorhinus xiaoheensis*" based on a single skull and mandible from the Yuanmou Basin. In "*A. xiaoheensis*", the skull roof narrows gradually toward the base of nasals, which are horizontal; the lingual cusps of the upper cheek teeth are only weakly constricted (Gao and Ma, 1997). The new specimens from the Yuanmou Basin differ from "*A. xiaoheensis*" in lacking these diagnostic features, although they resemble it in possessing closed parietal crests.

Zong (1998) erected *A. yuanmouensis* based on one slightly crushed skull from the Yuanmou Basin, China. Comparisons between the holotype of *A. yuanmouensis* and the new material described here reveal a set of shared diagnostic craniodental features: the occipital crest is much narrower than the paramastoid process; the parietal crests are prominent and closed, but do not fuse to form a sagittal crest; the posttympanic process expands transversely, and contacts the postglenoid process anteriorly; the nasal bone is short, and has an undulating dorsal profile; both lingual cusps are rounded and expanded; the antecrochet on each molars extends to the entrance of the median valley; the crista is doubled on each molars. These shared similarities justify referral of the new material to *A. yuanmouensis*.

Although the new specimens are referred to *A. yuanmouensis*, the phylogenetic status of this species remains uncertain. *A. yuanmouensis* resembles *Aceratherium incisivum* Kaup, 1832 in having the narrow parietal crests, and the shortened and undulated nasals (Kaup, 1832; Hünermann, 1989; Giaourtsakis and Heissig, 2004). However, the dorsal surface of the skull is abruptly constricted anterior to the orbit in *A. yuanmouensis*, distinct from the gradual constriction in *A. incisivum* (Giaourtsakis and Heissig, 2004). Another strong difference between the two genera is the possible presence of an I1 in *Aceratherium* (Hünermann, 1989).

Deng et al. (2013) established the species *Aceratherium porpani*, based on the skull and mandible from the latest Miocene in Tha Chang sand pits, Thailand. *A. porpani* shared several similarities with *A. yuanmouensis*: the nasal notch much retracted (P4/M1), the external auditory pseudomeatus closed, the constriction of the lingual cusps on the upper cheek teeth developed. The differences between these species, however, are more remarkable, the former having more derived skull features when compared with the latter: parietal crest separated widely, V-shaped notch on the occipital crest absent, and occipital crest widened laterally. Moreover, *A. yuanmouensis* has a crista on upper cheek teeth, which is absent on *A. porpani*.

Qiu (1979) assigned a crushed skull from the Late Miocene in Inner Mongolia, China, to *Aceratherium*, as "*Aceratherium*" *huadeensis*. Deng et al. (2013) revised it to *Acerorhinus*. This species displays the occlusal patterns of the upper cheek teeth similar to that of *A. yuanmouensis*, especially the expanded lingual cusps (Deng et al., 2013). On the other hand "*Aceratherium*" *huadeensis* differs from *A. yuanmouensis* and other species of *Acerorhinus* in having a set of particular craniodental features: the lingual cingulum on upper cheek teeth is completely reduced; the nasal notch is shallow (at the level P3); and the very broadly widened parietal crest.

Chilotherium Ringström, 1924 displays some diagnostic features that distinguish it from *A. yuanmouensis* and other species of *Acerorhinus*: the occipital crest is wide, making the nuchal face nearly square in outline; the parietal crest is concave; the zygomatic arches is always dorsoventrally shallower than that in *A. yuanmouensis*; the parastyle and the paracone rib on the upper cheek teeth are very poorly developed (Ringström, 1924; Deng, 2001a).

In the Chinese Late Miocene to Pliocene genus *Shansirhinus* Kretzoi, 1942 (Schlosser, 1903; Ringström, 1924, 1927; Tang et al., 1974; Qiu and Yan, 1982; Deng, 2005; Deng and Qi, 2009), the prominent parietal crests and dorsoventrally deep zygomatic arches are reminiscent of *A. yuanmouensis*. However, *A. yuanmouensis* lacks the well-developed enamel plications on the cristae and crochets of the upper cheek teeth, and the rugosity at the tip of the nasal, whereas both these characterized *Shansirhinus* (Deng, 2005). Deng (2005) suggested that *Shansirhinus* was the sister group of *Chilotherium* rather than *Acerorhinus*.

Qiu et al. (1987) highlighted the narrowness of the occipital crests relative to the posttympanic processes in *Acerorhinus*. Heissig (1989, 1999) noted that in *Acerorhinus* the skull roof is widest between the supraorbital processes and narrows abruptly toward the base of the nasals, and that the nasal notch is deep (at levels of P4-M1) and separated from the orbit by only a short distance. Deng and Qi (2009) also considered these features to be

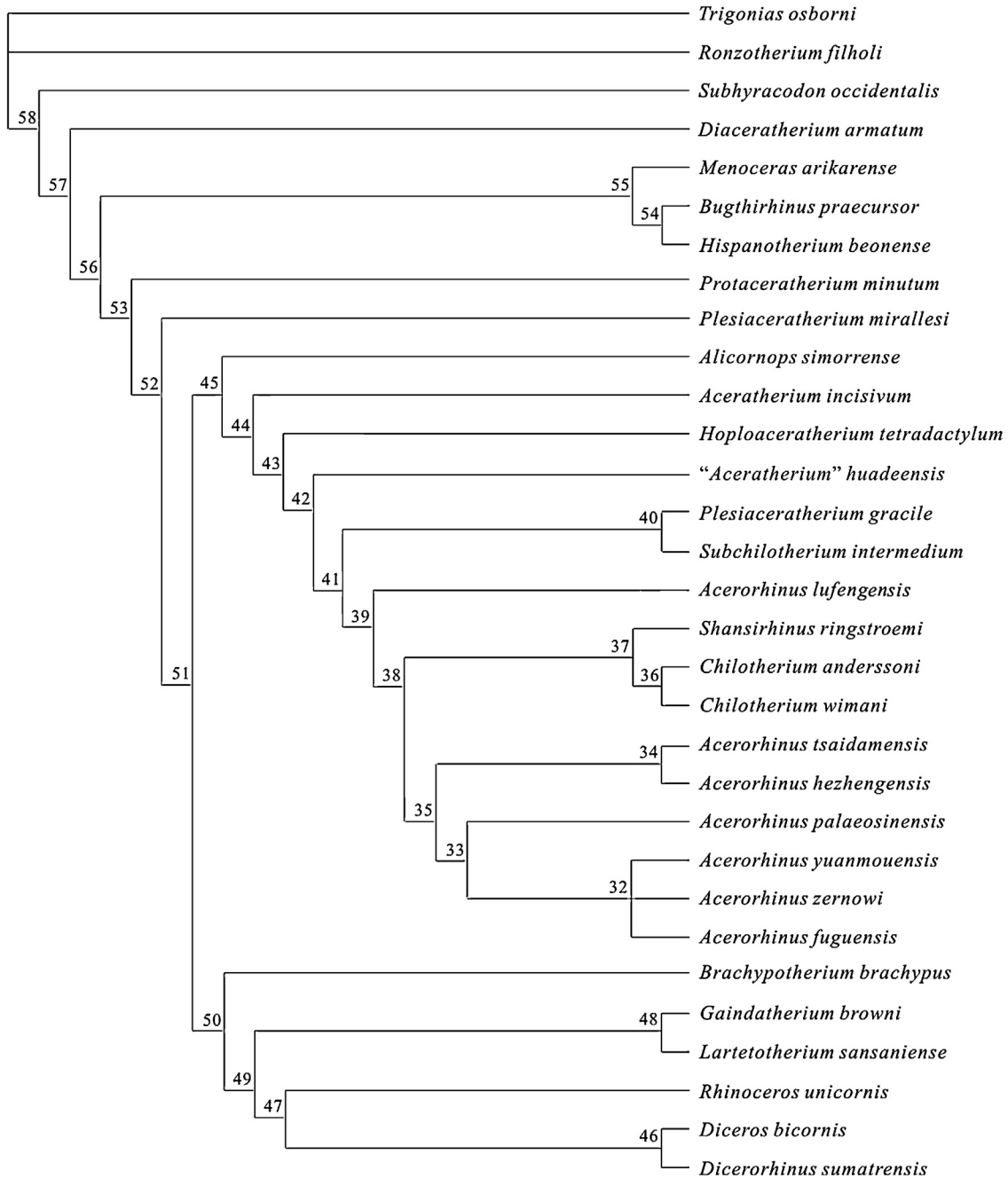

Fig. 6. Strict consensus tree of the two most parsimonious trees (tree length: 811 steps; CI = 0.32, RI = 0.55) obtained using PAUP 4.0β10 (heuristic search, branch-swapping TBR, 1000 replications with random taxa addition; Swofford, 2001), based on 214 craniodental characters, and performed on 31 terminal taxa, with *Trigonias osborni* as the outgroup. Ten characters have been treated as unordered: 2, 3, 8, 30, 31, 65, 94, 123, 131, and 170. Node numbers refer to the list of unambiguous synapomorphies (Appendix A-3).

typical of *Acerorhinus*. Accordingly, the presence of such features in the new specimens of *A. yuanmouensis* from the Yuanmou Basin, as well as in the holotype, confirms that this species should indeed be referred to *Acerorhinus*.

Six *Acerorhinus* species from China were recognized (Deng and Qi, 2009). With respect to skull morphology, *A. yuanmouensis* is more similar to *A. zernowi* than to other *Acerorhinus* species in displaying a marked ventral constriction of the zygomatic arches and a minimally developed postorbital process. Furthermore, *A. yuanmouensis* is an *Acerorhinus* species with the shortest nasal bones, whereas nasals of *A. palaeosinensis* (Ringström, 1924) and *A. hezhengensis* are much longer (Table 1). The posterior end of the nasal notch reaches the level of M1 in *A. yuanmouensis* (Zong, 1998), as in *A. fuguensis* (Deng, 2000), *A. tsaidamensis* (Bohlin, 1937), and *A. hezhengensis* (Qiu et al., 1987); this shared condition represents the greatest posterior extent of the notch seen in *Acerorhinus*. The postglenoid process extends farther ventrally than the paramastoid process in *A. yuanmouensis*, as in *A. zernowi* (Borissiak, 1915), *A. hezhengensis* (Qiu et al., 1987), and *A. fuguensis* (Deng, 2000).

The constrictions on the lingual cusps of the upper cheek teeth are much deeper in *A. yuanmouensis* than in *A. lufengensis* (Deng and Qi, 2009), closely resembling the condition in *A. hezhengensis* (Qiu et al., 1987). *A. lufengensis* has much wider upper cheek teeth than *A. yuanmouensis* and other species of *Acerorhinus* (Deng and Qi, 2009). The parastyle and the paracone rib in *A. yuanmouensis*

are more remarkable than in *A. hezhengensis*. The presence of cristae on the upper molars is variable among species of *Acerorhinus*, but *A. yuanmouensis* is the only one to have two cristae on M1 and M2. On the other hand, two intraspecific variations occur on the upper premolars of *A. yuanmouensis*, as in *A. tsaidamensis* (Bohlin, 1937): the lingual bridge seen in the upper premolars of IVPP V18565 is absent in the corresponding teeth of the holotype of *A. yuanmouensis*; a continuous lingual cingulum was present on the upper premolars of the holotype of *A. yuanmouensis* (Zong, 1998), but only traces of this structure can be seen on the corresponding teeth of IVPP V18565.

4. Discussion

Zong (1998) erected *A. yuanmouensis* based on a well-preserved skull. Deng (2000) referred this species to "*Acerorhinus xiaoheensis*" described by Gao and Ma (1997). Comparisons with other contemporaneous aceratheriines from the Late Miocene of Eurasia, and the results of a phylogenetic analysis based on 214 craniodental characters and thirty-one terminal taxa (Fig. 6), demonstrate that *A. yuanmouensis* is not a junior synonym of "*Acerorhinus xiaoheensis*". In the present analysis, *A. yuanmouensis* and five other species are gathered into the *Acerorhinus* clade, including the type species *A. zernowi* but excluding *A. lufengensis* (see below). *A. yuanmouensis* is distinguished from other species traditionally assigned to *Acerorhinus* by the presence of some specialized features, such as a short, undulating nasal bone and a V-shaped incision on the lingual cingulum of each upper premolar. Variations in the presence of the lingual bridge and the lingual cingulum on the upper premolars suggest an intra-specific trend toward reduction of both structures. The present analysis indicate that *A. yuanmouensis* has close affinities with *A. zernowi* and *A. fuguensis*, but recovers these three species in an unresolved soft trichotomy (Fig. 6) – morphological comparisons among all seven species of *Acerorhinus*, however, suggest that *A. yuanmouensis* and *A. zernowi* more closely related to each other than to *A. fuguensis*.

Deng and Qi (2009) established the species *A. lufengensis* based on some isolated cheek teeth and incisors. The lingual cusps of the upper cheek teeth of *A. lufengensis* are expanded, like those of other *Acerorhinus* species, and the constrictions are weak. However, it appears as the sister taxon of a [*Acerorhinus*, [*Shansirhinus*, *Chilotherium*]] clade in the present analysis (Fig. 6). Such contradiction in identity of *A. lufengensis* probably results from the limited amount of material available for this species. Before further discussion on the phylogenetic status of this species, its previously established taxonomic status should be reserved.

"*Aceratherium*" *huadeensis* is represented by one crushed skull with well-preserved but badly worn upper cheek teeth (Qiu, 1979). Deng et al. (2013) reassigned this species to *Acerorhinus*. It appears as the sister group of the [*Plesiaceratherium*, *Subchilotherium*, [*Acerorhinus lufengensis*, [*Acerorhinus*, [*Shansirhinus*, *Chilotherium*]]]] clade, and is not linked to either *Aceratherium* or the *Acerorhinus* clade. This species differs from both *Aceratherium* and *Acerorhinus* in that the lingual cingulum of upper premolars is completely reduced, and the nasal notch is moderately retracted. Its phylogenetic status remains unresolved in the present analysis (Fig. 6).

5. Conclusion

The present study describes new fossils from the Late Miocene of the Yuanmou Basin (Yunnan-Guizhou Plateau, Yunnan Province, China) and assigns them to *A. yuanmouensis*, a species previously reported from the same area. Morphological comparisons demonstrate that *A. yuanmouensis* is a valid species. Based on the results of a phylogenetic analysis involving 214 craniodental morphological characters scored for 31 terminal taxa, I confirm that this species belongs to *Acerorhinus* (Fig. 6).

The present analysis gives two additional interesting results regarding the genus *Acerorhinus*. First, the species *A. lufengensis*, represented by some isolated cheek teeth and incisors, is excluded from the genus *Acerorhinus*. Second, "*Aceratherium*" *huadeensis* is not related to either the genus *Aceratherium* or the genus *Acerorhinus*. The phylogenetic placement of both species will ultimately need to be reconsidered. However, I suggest that these species be retained in their current genera until their phylogenetic positions can be clarified by additional informative specimens.

Acknowledgements

We are very grateful to G.Q. Qi, who directed the field work together with J. Kelley and F. Gao and kindly provided the material for this study. We thank Profs. Z.X. Qiu., T. Deng, E. Cerdeño, and P.M. Butler for valuable comments on the manuscript. Special thanks must be extended to Z.J. Tseng and C. Sullivan for improving the language used in the manuscript. We are grateful to the technicians Y.M. Hou and Y. Xu for their work on the 3D reconstruction and illustration of the teeth P2-M2, respectively. This work was supported by the Strategic Priority Research Program of the Chinese Academy of Sciences (XDB03020104), and the Ministry of Science and Technology of China (2012CB821906).

Appendix A. Supplementary data

Supplementary information (cladistics analysis: analyzed taxa and character coding sources [A-1], list of character and character states [A-2], list of unambiguous synapomorphies [A-3], and character state data matrix [A-4]) associated with this article can be found, in the online version, at: http://dx.doi.org/10.1016/j.geobios.2013.10.001.

References

Antoine, P.-O., 2002. Phylogénie et évolution des Elasmotheriina (Mammalia, Rhinocerotidae). Mémoires du Muséum National d'Histoire Naturelle 188, 1–359.

Antoine, P.-O., Downing, K.F., Crochet, J.-Y., Duranthon, F., Flynn, L.J., Marivaux, L., Métais, G., Rajpar, A.R., Roohi, G., 2010. A revision of *Aceratherium blanfordi* Lydekker, 1884 (Mammalia: Rhinocerotidae) from the Early Miocene of Pakistan: Postcranials as a key. Zoological Journal of the Linnean Society 160, 139–194.

Antoine, P.O., Duranthon, F., Welcomme, J.L., 2003. *Alicornops* (Mammalia, Rhinocerotidae) dans le Miocène supérieur des collines Bugti (Balouchistan, Pakistan) : implications phylogénétiques. Geodiversitas 25, 575–603.

Bohlin, B., 1937. Eine Tertiäre Säugetier-Fauna aus Tsaidam. Palaeontologia Sinica C. New Series 14 (1) 1–111.

Borissiak, A., 1914. Mammifères fossiles de Sébastopol, I. Trudy Geolegicheskago Komiteta. Novaja Seria 87, 1–154 (in Russian).

Borissiak, A., 1915. Mammifères fossiles de Sébastopol, II. Trudy Geolegicheskago Komiteta. Novaja Seria 137, 1–45 (in Russian).

Cerdeño, E., 1996. Rhinocerotidae from the Middle Miocene of the Tung-gur Formation, Inner Mongolia (China). American Museum Novitates 3184, 1–43.

Deng, T., 2000. A new species of *Acerorhinus* (Perissodactyla, Rhinocerotidae) from the Late Miocene in Fugu, Shaanxi, China. Vertebrata PalAsiatica 38, 203–217.

Deng, T., 2001a. New materials of *Chilotherium wimani* (Perisodactyla, Rhinocerotidae) from the Late Miocene of Fugu, Shaanxi. Vertebrata PalAsiatica 39, 129–138.

Deng, T., 2001b. Cranial ontogenesis of *Chilotherium wimani* (Perissodactyla, Rhinocerotidae). In: Deng, T., Wang, Y. (Eds.), Proceedings of the Eighth Annual Meeting of the Chinese Society of Vertebrate Paleontology. China Ocean Press, Beijing, pp. 101–112.

Deng, T., 2005. New cranial material of *Shansirhinus* (Rhinocerotidae, Perissodactyla) from the Lower Pliocene of the Linxia Basin in Gansu, China. Geobios 38, 301–313.

Deng, T., 2006. Chinese Neogene mammal biochronology. Vertebrata PalAsiatica 44, 143–163.

Deng, T., Gao, F., 2006. Rhinocerotid fossils from the hominoid site in Yuanmou. Yunnan, China. In: Qi, G.Q., Dong, W. (Eds.), *Lufengpithecus hudienensis* Site. Science Press, Beijing, (in Chinese), pp. 188–195.

Deng, T., Hanta, R., Jintasakul, P., 2013. A new species of *Aceratherium* (Rhinocerotidae, Perissodactyla) from the Late Miocene of Nakhon Ratchasima, northeastern Thailand. Journal of Vertebrate Paleontology 33, 977–985.
Deng, T., Qi, G.Q., 2009. Rhinocerotids (Mammalia, Perissodactyla) from *Lufengpithecus* site, Lufeng, Yunnan. Vertebrata PalAsiatica 47, 135–152 (in Chinese).
Gao, F., Ma, B., 1997. Perissodactyla. In: He, Z.Q. (Ed.), Yuanmou Hominoid Fauna. Yunnan Science and Technology Press, Kunming, (in Chinese), pp. 106–111.
Giaourtsakis, I.X., Heissig, K., 2004. On the nomenclatural status of *Aceratherium incisivum* (Rhinocerotidae, Mammalia). Proceedings of the 5th International Symposium on Eastern Mediterranean Geology (Thessaloniki, Greece) 1, 314–317.
Goddard, J., 1970. Age criteria and vital statistics of a black rhinoceros population. African Journal of Ecology 8, 105–121.
Guérin, C., 1980. Les rhinocéros (Mammalia, Perissodactyla) du Miocène terminal au Pléistocène supérieur en Europe occidentale : comparaison avec les espèces actuelles. Documents du Laboratoire de Géologie de l'Université de Lyon, France, Sciences de la Terre 79, 1–1184.
Heissig, K., 1975. Rhinocerotidae aus dem Jungtertiär Anatoliens. Geologisches Jahrbuch B 15, 145–151.
Heissig, K., 1989. Rhinocerotidae. In: Prothero, D.R., Schoch, R.M. (Eds.), The Evolution of Perissodactyls. Oxford University Press, New York, pp. 399–417.
Heissig, K., 1999. Family Rhinocerotidae. In: Rössner, G.E., Heissig, K. (Eds.), The Miocene Land Mammals of Europe. Verlag Dr. Friedrich Pfeil, München, pp. 175–188.
Hillman-Smith, A.K.K., Owen-Smith, N., Anderson, J.L., Hall-Martin, A.J., Selaladi, J.P., 1986. Age estimation of the white rhinoceros (*Ceratotherium simum*). Journal of Zoology London 210, 357–359.
Hitchins, P.M., 1978. Age determination of the black rhinoceros (*Diceros bicornis* Linn.) in Zululand. South African Journal of Wildlife Research 8, 71–80.
Hünermann, K.A., 1989. Die Nashornskelette (*Aceratherium incisivum* Kaup, 1832) aus dem Juntertiajouterär vom Höwenegg im Hegau (Südwestdeutschland). Andrias 6, 5–116.
Jiang, C., 1996. Preliminary study of the upper jaw fossils of hominoids from Xiaohe Village in Yuanmou County. Acta Anthropological Sinica 15, 36–40 (in Chinese).
Jiang, C., Lin, X., Li, J.M., 1993. Hominoid teeth from Leilao in Yuanmou, Yunnan. Acta Anthropologica Sinica 12, 97–103 (in Chinese).
Jiang, N.R., Sun, R.L., Liang, Q.Z., 1987. Discovery and significance of early stage pithecanthrope (tooth fossil) in Yuanmou Basin. Yunnan Geology 6, 157–162 (in Chinese).
Jiang, Z.W., 1997. General Geography. In: He, Z.Q. (Ed.), Yuanmou Hominoid Fauna. Yunnan Science and Technology Press, Kunming, (in Chinese), pp. 1–8.
Kaup, J.J., 1832. Über *Rhinoceros incisivus* Cuvier und eine neue Art *Rhinoceros schleiermacheri*. Isis 8, 898–904.
Kelley, J., Gao, F., 2012. Juvenile hominoid cranium from the late Miocene of Southern China and hominoid diversity in Asia. Proceedings of the National Academy of Sciences, USA 109, 6882–6885.
Kretzoi, M., 1942. Bemerkungen zum system der nachmiozänen Nashorn-Gattungen. Földtani Közlöny 72, 4–12.
Lucas, F.A., 1901. A new rhinoceros, *Trigonias osborni* from the Miocene of South Dakota. Proceedings of the United States National Museum 23, 221–223.
Lydekker, R., 1881. Indian Tertiary and Post-Tertiary vertebrata, Siwalik Rhinocerotidae. Memoirs Geological Survey of India, Palaeontologia Indica Series 10 (11) 1–62.
Ni, X.J., Qiu, Z.D., 2002. The micromammalian fauna from the Leilao, Yuanmou hominoid locality: implication for biochronology and paleoecology. Journal of Human Evolution 42, 535–546.
Pan, Y.R., 1997. Mammalia, Artiodactyla and Primates. In: He, Z.Q. (Ed.), Yuanmou Hominoid Fauna. Yunnan Science and Technology Press, Kunming, (in Chinese), pp. 114–120.
Prothero, D.R., Schoch, R.M., 1989. Rhinocerotidae. In: Prothero, D.R., Schoch, R.M. (Eds.), The Evolution of Perissodactyls. Oxford University Press, New York, pp. 530–537.
Qi, G.Q., Dong, W., Zheng, L., Zhao, L.X., Gao, F., Yue, L.P., Zhang, Y.X., 2006. Taxonomy, age and environment status of the Yuanmou hominoids. Chinese Science Bulletin 51, 833–841 (in Chinese).
Qiu, Z.D., 1979. Some mammalian fossils from the Pliocene of Inner Mongolia and Gansu (Kansu). Vertebrata PalAsiatica 17, 222–235.
Qiu, Z.X., Xie, J.Y., Yan, D.F., 1987. A new chilothere skull from Hezheng, Gansu, China, with special reference to the Chinese "Diceratherium". Scientia Sincia B5, 545–552.
Qiu, Z.X., Qiu, Z.D., 1995. Chronological sequence and subdivision of Chinese Neogene mammalian faunas. Palaeogeography, Palaeoclimatology, Palaeoecology 116, 41–70.
Qiu, Z.X., Yan, D.F., 1982. A horned *Chilotherium* skull from Yushe, Shansi. Vertebrata PalAsiatica 20, 122–132 (in Chinese).
Ringström, T., 1924. Nashörner der *Hipparion*-fauna Nord-Chinas. Palaeontologia Sinica Series 1 (4) 1–159.
Ringström, T., 1927. Über Quartäre und Jungtertiäre Rhinocerotiden aus China und der Mongolei. Palaeontologia Sinica New Series C 4 (3) 1–21.
Schlosser, M., 1903. Die fossilen Säugethiere Chinas nebst einer Odontographie der recenten Antilopen. Abhandlungen der Koniglichen Bayerischen Akademie der Wissenschaften 22, 1–221.
Sisson, S.B., 1953. The Anatomy of the Domestic Animals, fourth ed. Saunders W.B. Company, Philadelphia and London, 1–972.
Steininger, F.F., 1999. Chronostratigraphy, geochronology and biochronology of the Miocene European Land Mammal Mega-Zones (ELMMZ) and the Miocene Mammal-Zones (MN-Zones). In: Rössner, G.E., Heissig, K. (Eds.), The Miocene Land Mammals of Europe. Verlag Dr. Friedrich Pfeil, München, pp. 9–24.
Swofford, D.L., 2001. PAUP* (phylogenetic analysis using parsimony [*and other methods] version 4.0β10) Sinauer, Sunderland, MA.
Tang, Y.J., You, Y.Z., Liu, H.Y., Pan, Y.R., 1974. New materials of Pliocene mammals from Banguo Basin of Yuanmou, Yunnan and their stratigraphical significance. Vertebrata PalAsiatica 12, 60–67 (in Chinese).
Yan, D.F., Heissig, K., 1986. Revision and autopodial morphology of the Chinese-European rhinocerotid genus *Plesiaceratherium* Young, 1937. Zitteliana 14, 81–110.
Young, C.C., 1937. On a Miocene mammalian fauna from Shantung. Bulletin of the Geological Society of China 17, 209–255.
Yue, L.P., Zhang, Y.X., Qi, G.Q., Heller, F.A., Wang, J.Q., Yang, L.R., Zhang, R., 2004. Paleomagnetic age and palaeobiological significance of hominoid fossil strata of Yuanmou Basin in Yunnan. Science China D 47, 405–411 (in Chinese).
Zhang, Y.X., Zheng, L., Ji, X.P., Zhang, J.H., 2002. Taphonomy of the hominoid fauna in the Yuanmou Basin, Yunnan. Acta Geologica Sinica 76, 45–49 (in Chinese).
Zong, G.F., 1998. A new evidence of dividing in the Neogene stratigraphy of Yuanmou Basin. Memories of Beijing Nature History Museum 56, 159–178 (in Chinese).